The following publication Z. Situ, I. W. -H. Ho, T. Wang and S. C. Liew, "An ICI-Aware Approach for Physical-Layer Network Coding in Time-Frequency-Selective Vehicular Channels," 2018 IEEE 87th Vehicular Technology Conference (VTC Spring), Porto, Portugal, 2018 is available at https://doi.org/10.1109/VTCSpring.2018.8417525.

An ICI-aware Approach for Physical-layer Network Coding in Time-frequency-selective Vehicular Channels

Zhenhui Situ*, Ivan Wang-Hei Ho*†, Taotao Wang‡, and Soung Chang Liew‡
*Department of Electronic and Information Engineering, The Hong Kong Polytechnic University, Hong Kong
†Research Institute for Sustainable Urban Development, The Hong Kong Polytechnic University, Hong Kong
‡Department of Information Engineering, The Chinese University of Hong Kong, Hong Kong
Email: z.situ@connect.polyu.hk, ivanwh.ho@polyu.edu.hk, ttwang@ie.cuhk.edu.hk, soung@ie.cuhk.edu.hk

Abstract*—Applying physical-layer network coding (PNC) to vehicular ad-hoc networks (VANETs) can theoretically boost the network throughput by 100%, thus partially addressing the intermittent node connectivity and short contact time issues caused by high speed vehicle motions. However, the application of OFDM modulated PNC in VANETs faces detrimental effects caused by carrier frequency offsets (CFOs) and time-frequency-selective channels. CFOs may destroy the orthogonality of OFDM subcarriers, resulting in inter-carrier interference (ICI). The CFOs of two transmitters may also be different, and cannot be removed by CFO tracking and equalization at the receiver as in conventional single-user communication even if the CFOs are known. In addition, time-frequency-selective channels due to delay and Doppler spreads are difficult to estimate and non-accurate channel estimations will increase the detection bit error rate (BER). To address the two challenges, this paper proposes an ICI-aware approach that jointly exploits pilot and data for channel estimation and data detection. Specifically, our approach jointly uses the belief propagation (BP) algorithm to mitigate the CFO/ICI effect for data detection, and the expectation maximization (EM) algorithm to accurately estimate the channels. A linear interpolation method and an ICI compensation method are simulated as benchmarks. Simulation results indicate that our approach improves the BER performance compared to the two benchmarks (more than 2 dB SNR gain in most cases), especially in the high SNR regime.

I. Introduction

Vehicular Ad-hoc Networks (VANETs) are attracting increasing attentions in both academia and industry. VANETs can enhance traffic safeties and provide diverse services by enabling information exchange among vehicles. Sophisticated applications like self-driving also require the support of VANETs to satisfy the demand of low latency communications. The IEEE 802.11 family assigns the 5.9 GHz band (5.85-5.925 GHz) and customizes the 802.11p standard for Vehicle-to-X (V2X) communications. OFDM continues to be the preferred modulation scheme in this standard..

Many scenarios in VANETs call for the data between two end nodes to be forwarded through a relay node (e.g., road side unit that relays data between vehicles). Such a relay channel faces many challenges, including intermittent node connectivity and short contact time between nodes induced by vehicular mobilities [1], [2]. A strategy to address the challenges is to improve the throughput so that more data can be transmitted within a short duration. Thus motivated, [1] proposed the application of physical-layer network coding (PNC) [3] in VANETs. However, the study did not consider that the imperfect channel state information (CSI) will degrade the detection accuracy. Moreover, we found that the prior state-of-the-art PNC receivers did not provide a robust channel estimator against time-frequency-selective vehicular channels.

Fig. 1 shows a two-way relay channel (TWRC) operated with OFDM modulated PNC. Two semi-automated cars A and

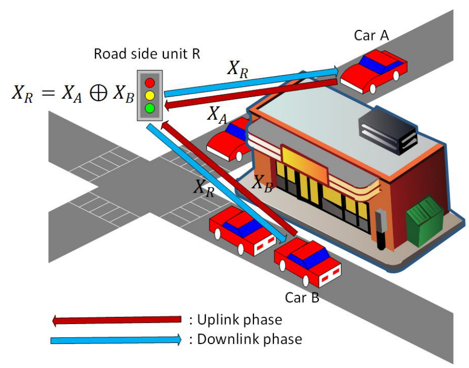

Fig. 1. An TWRC that operates with OFDM modulated PNC.

B try to exchange traffic information within their detection range. Obstructed by the buildings, the two cars communicate via a relay R and the data exchange is divided into an uplink phase and a downlink phase. In the uplink phase, the two end nodes simultaneously transmit signals X_A and X_B to relay R via channels A and B respectively. After receiving the overlapped signal and decoding the signal, relay R obtains the exclusive or (XOR) output of the received signals, X_R, and broadcasts X_R in the downlink phase. Finally, two end nodes recover their desired data form received X_R and self information.

Theoretically, PNC can increase throughput by 100% in TWRC, compared with conventional multi-hop wireless communications. However, OFDM modulated PNC systems are sensitive to the carrier frequency offset (CFO) between the two end nodes. The CFO is originated from imperfect local oscillators at the two nodes and Doppler shifts due to motions. CFO leads to inter-carrier interferences (ICI) among OFDM subcarriers (ICI degrades the symbol-by-symbol XOR detection). This negative effect of CFO is inevitable in OFDM modulated PNC systems since the CFOs from multi transmitters may be different, and thus cannot be removed by conventional CFO tracking and equalization [4], [5]. Besides the CFO problem, channel estimation in PNC is particularly challenging owing to the superimposed signals and time-frequency-selective channels [6]. Moreover, when OFDM modulated PNC is applied in VANETs, the two problems are compounded by the high mobility of vehicles. For the channel estimation, [6] customized a joint channel estimation and channel decoding framework for PNC, but it only considered single-carrier systems without CFO and the channel was frequency-flat. For OFDM PNC, [7] adopted time-orthogonal (time non-overlapping) training symbols and pilots for the two end nodes. Therefore, the channel estimation problem in PNC is reduced to that of traditional single-user communication systems. A common method to mitigate ICI induced by CFO is interference cancellations. For example, [8]–[10] used iterative interference cancellations and signal detection/decoding, they focused on CFO but assumed the channel to be known. So far, the priori PNC receivers did not provide the solution against time-frequency-selective vehicular channels, and they preferred to either ignore or compensate the ICI. In contrast, we exploit an ICI-aware method to tackle the ICI and design a robust PNC receiver for time-frequency-selective vehicular channels.

Compared with previous works, this paper addresses two critical issues in VANETs: the channel estimation under time-frequency-selective channels and the signal detection under ICI. We propose an ICI-aware approach to solve the two problems jointly. The salient features of the proposed approach are as follows:

1) We use the expectation maximization (EM) algorithm to extract channel information contained in both pilots and data, taking into consideration the ICI induced by CFO.
2) We exploit the belief propagation (BP) algorithm and an ICI-aware method to mitigate the detrimental effects of CFO in the signal detection.
3) The proposed approach iterates between 1) and 2) to improve the channel estimation and signal detection progressively.

Benefit from the proposed approach, the further works w.r.t PNC in VANETs are possible. For instance, the channel coding design can ignore ICI since it can be removed by the proposed approach, and higher level design (e.g. MAC layer) is feasible with the support from robust physical-layer receiver.

The remainder of this paper is organized as follows. The system model is described in Section II. In Section III, the proposed ICI-aware approach is discussed in detailed. After that, simulation results are presented in Section IV. Finally, Section V concludes the paper.

II. System model

We assume that the signals in the uplink phase undergo time-frequency-selective channels characterized by wide-sense stationary uncorrelated scattering (WSSUS) models [11]. The time-variant impulse response of the channel between the relay and node i can be interpreted as

$$h_i(\tau_i,t)=\sum_{p_i=1}^{P_i} c_{p_i}(t)\delta(\tau_i-\tau_{p_i}) \tag{1}$$

where $i\in\{A,B\}$, P_i is the total number of propagation paths. For the p_i-th path with delay τ_{p_i}, the complex channel gain $c_{p_i}(t)$ is modeled as a Rayleigh process and follows the Jakes' power spectrum [11] with maximum Doppler frequency f_{d_i}.

$$f_{d_i}=\frac{v_i}{c}f_c \tag{2}$$

where c is the speed of electromagnetic waves, f_c is the carrier frequency, and v_i is the relative velocity between the transmitter and receiver. Besides the Doppler spread, the imperfection of the local oscillators used to generate the RF carrier leads to frequency offsets f_{δ_i}, $i\in\{A,B\}$.

For OFDM, the number of subcarriers is M and the length of the cyclic prefix (CP) is G. In this paper, we assume CP can successfully eliminate inter-symbol interference (ISI). Let the bandwidth be B and the sampling rate is $B=1/T_s$, where T_s is the sampling interval. Each frame contains L symbols. After OFDM modulation, the transmitted time-domain baseband discrete signal from node i at the l-th symbol is represented as

$$x_i[q{+}G{+}(l{-}1)(M{+}G)]=\frac{1}{M}\sum_{m=-M/2}^{M/2-1} X_{i,l}[m]e^{j2\pi\frac{m}{M}q} \tag{3}$$

where q is the time index within the symbol, and $X_{i,l}[m]$ is the modulated symbol. The baseband signals from nodes A and B overlap at the relay R as

$$y(t)=\sum_{i\in\{A,B\}}(x_i(t)\otimes h_i(\tau_i,t))e^{j2\pi f_{\delta_i}t}+n(t) \tag{4}$$

where $\otimes$ denotes the convolution operation, $n(t)$ is the complex white Gaussian noise with zero mean and variances σ_t^2. Here we further consider the product of $h_i(\tau_i,t)$ and $e^{j2\pi f_{\delta_i}t}$ to be one component $h_i(\tau_i,t)$ since the hardware frequency offset can be regarded as part of the Doppler spread without loss of generality. After performing the FFT operation, the signal of the l-th symbol can be expressed as:

$$\boldsymbol{Y}_l=\boldsymbol{H}_{A,l}\boldsymbol{X}_{A,l}+\boldsymbol{H}_{B,l}\boldsymbol{X}_{B,l}+\boldsymbol{W}_l \tag{5}$$

Here we use bold capital letters to denote arrays (e.g., vector or matrix). $\boldsymbol{Y}_l$ and $\boldsymbol{X}_{i,l}$ are $M\times 1$ vectors containing data information of M subcarriers, $\boldsymbol{W}_l$ is a $M\times 1$ vector containing the noise on each subcarriers, and the noise is zero mean with variance $\sigma_f^2=M\sigma_t^2$. $\boldsymbol{H}_{i,l}$ is an $M\times M$ matrix, the diagonal elements $\boldsymbol{H}_{i,l}[m,m]$ denote complex channel responses for desired signals on the target subcarriers, while other elements are coefficients for ICI. The impulse response from subcarrier k to subcarrier m is given by

$$
\begin{aligned}
\boldsymbol{H}_{i,l}[m,k] &= \sum_{p_i=1}^{P_i} \alpha_t(m,k,l,p_i) e^{-j2\pi k \Delta f \tau_{p_i}} \\
\alpha_t(m,k,l,p_i) &= \sum_{q=0}^{M-1} c_{p_i}((q+G)T_s + (l-1)T) e^{j2\pi \frac{k-m}{M} q}
\end{aligned}
\tag{6}
$$

$\alpha_t(m,k,l,p_i)$ is the output coefficient of the signal on the k-th subcarrier to the m-th subcarrier at the l-th symbol. Delay τ_{p_i} also causes a phase rotation $e^{-j2\pi k\Delta f \tau_{p_i}}$, where $\Delta f = 1/(MT_s)$ is the subcarrier spacing. Previous work [12] regards ICI as part of the noise, but here we attempt to implement an ICI-aware method to mitigate the negative effect of CFO. We use a polynomial basis expansion model (P-BEM) [13] to approximate the channels for VANETs. With P-BEM, the complex channel gain $c_{p_i}(t)$ can be expressed as

$$
c_{p_i}(qT_s) = \sum_{g=1}^{G_z} \theta_{p_i,g} q^{g-1} + \xi[q] \tag{7}
$$

where $\theta_{p_i,g}$ is a polynomial coefficient to build the target channels, and $\xi[q]$ is the approximation error. Once all the polynomial coefficients are known, we can calculate the channel gain $c_{p_i}(qT_s)$, and thus, the output coefficient $\alpha_t(k,z,m,p_i)$ can be estimated. If the delay spread τ_{p_i} is also known, we can completely reconstruct the impulse response matrix $\boldsymbol{H}$. Applying P-BEM in (6), we have

$$
\begin{aligned}
\boldsymbol{H}_{i,l}[m,k] = \sum_{p_i=1}^{P_i} \sum_{g=1}^{G_z} \{ e^{-j2\pi k\Delta f \tau_{p_i}} \sum_{q=0}^{M-1} ((q+G)T_s \\
+ (l-1)T)^{g-1} e^{j2\pi \frac{k-m}{M} q} \} \theta_{p_i,g}
\end{aligned}
\tag{8}
$$

Then we can re-write the impulse response to be

$$
\begin{aligned}
\boldsymbol{H}_{i,l}[m,k] =& \boldsymbol{\alpha}(m,k,l,i)\boldsymbol{\theta}_i \\
\boldsymbol{\alpha}(m,k,l,i) =& [\alpha_{p_1,1}(m,k), \alpha_{p_1,2}(m,k), ..., \alpha_{p_1,G_z}(m,k), \\
& \alpha_{p_2,1}(m,k), ..., \alpha_{P_i,G_z}(m,k)] \\
\alpha_{p_i,g}(m,k) =& e^{-j2\pi k\Delta f \tau_{p_i}} \\
& \sum_{q=0}^{M-1} ((q+G)T_s + (l-1)T)^{g-1} e^{j2\pi \frac{k-m}{M} q} \\
\boldsymbol{\theta}_i =& [\theta_{p_1,1}, \theta_{p_1,2}, ..., \theta_{p_1,G_z}, \theta_{p_2,1}, ..., \theta_{P_i,G_z}]^T
\end{aligned}
\tag{9}
$$

The proposed approach estimates the paths with delay from zero to $N_{\tau_i} - 1$ sampling intervals to approximate the delay spread. Therefore, $\boldsymbol{\theta} = [\boldsymbol{\theta}_A, \boldsymbol{\theta}_B]$ and $\boldsymbol{H}$ are equivalent, and they denote the channel information in the remainder of this paper.

III. PROPOSED ICI-AWARE APPROACH

The proposed approach focuses on addressing two problems. The first task is to perform channel estimation with pilot and data tones. The second task is to detect the transmitted data $\boldsymbol{X} = [X_A, X_B]^T$ given channel information $\boldsymbol{H}$ and received data $\boldsymbol{Y}$. $\boldsymbol{X}$ is a three dimensional array containing element $\boldsymbol{X}_{i,l}[m]$. Similarly, $\boldsymbol{Y}$ is a two dimensional matrix including element $\boldsymbol{Y}_l[m]$ and $\boldsymbol{H}$ is a four dimensional array containing element $\boldsymbol{H}_{i,l}[m,k]$. Accordingly, the proposed approach can be divided into two phases:

Channel estimation phase: to obtain the optimal channel information with the maximum a posteriori (MAP) probability $\hat{\boldsymbol{H}}_{MAP} = \arg\max_{\boldsymbol{H}} \sum_{\boldsymbol{X}} p(\boldsymbol{H}, \boldsymbol{X}|\boldsymbol{Y})$. The EM algorithm is applied in this phase.

Signal detection phase: given the MAP $\hat{\boldsymbol{H}}_{MAP}$, to find the MAP probability $p(\boldsymbol{X}|\hat{\boldsymbol{H}}_{MAP}, \boldsymbol{Y})$. The BP algorithm is used in this phase.

The proposed approach iterates between the two phases.

A. Signal detection phase

Given the estimated channel information $\boldsymbol{H}$, signal detection is implemented in each symbol individually. When CFO exists, the received signal on one subcarrier suffers ICI from other subcarriers. In this work, we take the effect of ICI into account. A Markov network for one received symbol, which is shown in Fig. 2, is constructed and the sum-product BP algorithm is applied to conduct the inference to obtain the marginal probability of the transmitted data. Each received

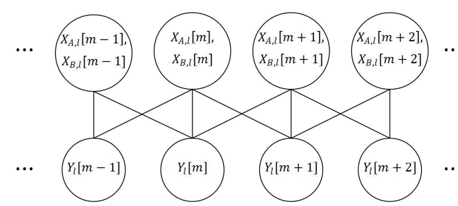

Fig. 2. The Markov network for signal detection.

signal $\boldsymbol{Y}_l[m]$ is connected to the corresponding subcarrier and two neighboring subcarriers. The reason why only three subcarriers are connected here is that according to our studies in [5], the received signal on one subcarrier mainly depends on the desired signal on the subcarrier and the ICI from two adjacent subcarriers. Rather than individual signal estimation, this work considers joint signal detection, and thus retains the correlation between the data from the two end nodes. The joint probability density function (pdf) of data from three successive subcarriers can be calculated as

$$
\begin{aligned}
& p(\boldsymbol{X}_l[m-1], \boldsymbol{X}_l[m], \boldsymbol{X}_l[m+1] | \boldsymbol{Y}_l[m], \boldsymbol{H}_l) \propto \\
& \exp\{-|\boldsymbol{Y}_l[m] - \sum_i \sum_{u=m-1}^{m+1} \boldsymbol{H}_{i,l}[m,u] \boldsymbol{X}_{i,l}[u]|^2 / 2\sigma_f^2\}
\end{aligned}
\tag{10}
$$

where $\boldsymbol{X}_l[m]$ denotes $\{\boldsymbol{X}_{A,l}[m], \boldsymbol{X}_{B,l}[m]\}$ and $\boldsymbol{H}_l$ is $\{\boldsymbol{H}_{A,l}, \boldsymbol{H}_{B,l}\}$. The factor $\boldsymbol{Y}_l[m]$ contains the joint pdf $p(\boldsymbol{X}_l[m-1], \boldsymbol{X}_l[m], \boldsymbol{X}_l[m+1] | \boldsymbol{Y}_l[m], \boldsymbol{H}_l)$. Then the marginal probability of $\boldsymbol{X}_l[m]$ can be obtained with the BP algorithm. Since the joint pdf of received data is required in the channel estimation phase, this paper applies the sum-product message passing algorithm to conduct the inference. Specifically, each $\boldsymbol{Y}$ factor passes self information to neighboring $\boldsymbol{Y}$ factors. After that, each $\boldsymbol{Y}$ factor calculates the belief as follows:

$$\begin{aligned} & Belief_m \\ = & \prod_{k \in \{m-1, m, m+1\}} p(\boldsymbol{X}_l[k-1], \boldsymbol{X}_l[k], \boldsymbol{X}_l[k+1] | \boldsymbol{Y}_l[k], \boldsymbol{H}_l) \end{aligned} \tag{11}$$

After performing marginalization, the marginal probability is obtained as the output of the signal detection phase.

In addition, the pdf output of signal detection can be further improved via channel coding. We have implemented channel coding on the proposed approach and the results will be shown in Section IV.

B. Channel estimation phase

Due to the time-frequency-selective channels and the effect of ICI, it is difficult to track the channel information with pilots only. The solution is to make use of data tones to enhance the channel estimation. The EM algorithm is applied to estimate the channel. There are three steps as follows: 1) Initialization step: find the initial channel information $\boldsymbol{H}^{init}$; 2) Expectation step (E-step): given the previous estimation $\boldsymbol{H}^{old}$, evaluate the auxiliary function

$$Q(\boldsymbol{H}|\boldsymbol{H}^{old}) = \sum_{\boldsymbol{X}} p(\boldsymbol{X}|\boldsymbol{Y}, \boldsymbol{H}^{old}) \log p(\boldsymbol{X}, \boldsymbol{Y}|\boldsymbol{H}) \tag{12}$$

3) Maximization step (M-step): re-estimate the channel

$$\boldsymbol{H}^{new} = \arg\max_{\boldsymbol{H}} Q(\boldsymbol{H}|\boldsymbol{H}^{old}) \tag{13}$$

Here, we re-write the auxiliary function in E-step:

$$Q(\boldsymbol{H}|\boldsymbol{H}^{old}) \propto \sum_{\boldsymbol{X}} p(\boldsymbol{X}|\boldsymbol{Y}, \boldsymbol{H}^{old}) \log p(\boldsymbol{Y}|\boldsymbol{X}, \boldsymbol{H}) \tag{14}$$

where $p(\boldsymbol{X}|\boldsymbol{Y}, \boldsymbol{H}^{old})$ is the posteriori probability which can be calculated based on the signal detection phase. And the auxiliary function is equal to the summation of sub-auxiliary functions of individual symbols as

$$Q(\boldsymbol{H}|\boldsymbol{H}^{old}) = \sum_{l=1}^{L} Q(\boldsymbol{H}_l|\boldsymbol{H}_l^{old}) \tag{15}$$

It turns out that the global auxiliary function can be divided into multiple sub-auxiliary functions, and the sub-auxiliary functions for individual symbols can be calculated based on theirs corresponding posteriori probability. In the proposed approach, channel estimation runs in each group consisting of G_z successive symbols. For each group, the Q function is equal to the sum of G_z sub-auxiliary functions as follows:

$$\begin{aligned} Q(\boldsymbol{H}|\boldsymbol{H}^{old}) \propto & \sum_{g=1}^{G_z} \sum_{\boldsymbol{X}_g} \sum_{m=-M/2}^{M/2-1} p(\boldsymbol{X}_g|\boldsymbol{Y}, \boldsymbol{H}^{old}) \\ \{-|\boldsymbol{Y}_g[m] - & \sum_i \sum_{k=-M/2}^{M/2-1} \boldsymbol{H}_{i,g}[m,k] \boldsymbol{X}_{i,g}[k]|^2 / (2\sigma_f^2)\} \end{aligned} \tag{16}$$

Then, we apply the P-BEM and re-write $\boldsymbol{H}_{i,g}[m,k]$ according to (9).

$$\begin{aligned} & Q(\boldsymbol{H}|\boldsymbol{H}^{old}) \\ \propto & \sum_{g=1}^{G_z} \sum_{\boldsymbol{X}_g} \sum_{m=-M/2}^{M/2-1} p(\boldsymbol{X}_g|\boldsymbol{Y}, H^{old}) \{-|\boldsymbol{Y}_g[m] - \{ \sum_{k=-M/2}^{M/2-1} \\ & [\boldsymbol{\alpha}(m,k,g,A) \boldsymbol{X}_{A,g}[k], \boldsymbol{\alpha}(m,k,g,B) \boldsymbol{X}_{B,g}[k]]\} \\ & [\boldsymbol{\theta}_A, \boldsymbol{\theta}_B]^T|^2 / (2\sigma_f^2)\} \end{aligned} \tag{17}$$

To maximize the Q function, we make the associated derivative to be zero as

$$\begin{aligned} 0 = \frac{dQ(\boldsymbol{H}|\boldsymbol{H}^{old})}{d\boldsymbol{\theta}} = & \sum_{g=1}^{G_z} \sum_{m=-M/2}^{M/2-1} (\boldsymbol{Y}_g[m] - \{ \sum_{k=-M/2}^{M/2-1} \\ & [\boldsymbol{\alpha}(m,k,g,A) \boldsymbol{X}_{A,g}^{\hat{}}[k], \boldsymbol{\alpha}(m,k,g,B) \boldsymbol{X}_{B,g}^{\hat{}}[k]]\} \boldsymbol{\theta}^T) \end{aligned} \tag{18}$$

where $\boldsymbol{X}_{i,g}^{\hat{}}[k]$ is the expected data. Thus, the EM algorithm can be regarded as the problem of finding the optimal $\boldsymbol{\theta}$ to minimize the error in (18). Here, we utilize a minimum mean square error (MMSE) estimator to identify.

$$\boldsymbol{\theta}^{new} = (\boldsymbol{A}_G + \boldsymbol{\Sigma}_n (\boldsymbol{A}_G^H)^{-1} \boldsymbol{\Sigma}_{\boldsymbol{\theta}}^{-1})^{-1} \boldsymbol{Y}_G \tag{19}$$

where $\boldsymbol{Y}_G$ is a $(MG_z) \times 1$ vectors containing the received data of a group, $\boldsymbol{A}_G$ is a $\{MG_z\} \times \{(P_A + P_B)G_z\}]$ matrix, each row in $\boldsymbol{A}_G$ contains a vector $\sum_{k=-M/2}^{M/2-1} [\boldsymbol{\alpha}(m,k,g,A) \boldsymbol{X}_{A,g}^{\hat{}}[k], \boldsymbol{\alpha}(m,k,g,B) \boldsymbol{X}_{B,g}^{\hat{}}[k]]$. $\boldsymbol{\Sigma}_n$ and $\boldsymbol{\Sigma}_\theta$ are the covariance matrices of noise and $\boldsymbol{\theta}$, respectively. The diagonal elements in $\boldsymbol{\Sigma}_n$ are $2\sigma_f^2$ and other elements are zero. Since all paths in the channel model are uncorrelated, $\boldsymbol{\Sigma}_{\boldsymbol{\theta}}$ is a diagonal matrix and the k-th diagonal element is $E(|\boldsymbol{\theta}[k]|^2)$. In each iteration of the EM algorithm, we use the channel estimation result from the previous iteration to calculate $\boldsymbol{\Sigma}_{\boldsymbol{\theta}}$. Unlike ICI compensation or equalization, the proposed channel estimation takes ICI into consideration and evaluate the optimal $\boldsymbol{\theta}$, then the $\boldsymbol{H}$ array can be established based on $\boldsymbol{\theta}$. Therefore, it is ICI-aware channel estimation.

For the initialization step, we only use the pilots to implement channel estimation, it is easy to achieve by removing the data tones in (18). In addition, the covariance matrix $\boldsymbol{\Sigma}_{\boldsymbol{\theta}}$ is regarded as an identity matrix at the beginning.

IV. Simulation results

There are two input variables in the simulations: the maximum Doppler frequency and the signal-to-noise ratio (SNR). Under different input conditions, the approach is evaluated based on bit error rate (BER) of the decoded XOR data at the relay. We consider a five-path Rayleigh fading channel for both nodes A and B. The fading spectral shapes of all paths are Jakes' power spectrum with the same maximum Doppler frequency. In terms of the delay spread and the path power, we apply the parameters of RTV-Urban Canyon and Canyon Oncoming cases [14]. For node B, we further add 100 ns delay and -3 dB power for all paths. The channel parameters are listed in Table I. In terms of the hardware frequency offset, we set $f_{\delta_A} = 1250$ Hz and $f_{\delta_B} = -1250$ Hz according to our empirical measurement. The simulations are designed based on

TABLE I
TIME-FREQUENCY-SELECTIVE CHANNEL PARAMETERS

Path no.	Power (A)	Delay (A)	Power (B)	Delay (B)
1	0 dB	0 ns	-3 dB	100 ns
2	-11.5 dB	100 ns	-13.0 dB	201 ns
3	-19.0 dB	200 ns	-20.8 dB	301 ns
4	-25.6 dB	300 ns	-24.1 dB	400 ns
5	-28.1 dB	500 ns	-29.3 dB	500 ns

the 802.11p standard. The bandwidth B is configured to be 10 MHz. Both BPSK and QPSK modulations are considered. The number of subcarriers is 144 including 120 data tones and 24 pilot tones. The 24 pilot tones are uniformly inserted among all subcarriers, one half of 24 pilots is assignment to node A and the other half is assigned to node B. The CP length G is set to be nine. For each frame, we have 126 symbols and each group contains two symbols. The number of evaluated paths N_{τ_i} is configured to be six for the two end nodes. The maximum number of iterations in the EM algorithm is five and the results of each iteration are evaluated. We consider the same normalized maximum Doppler frequency $f/\Delta f$ for both node A and B. In the simulations, we set $f/\Delta f$ to be 0.05 and 0.1, and under these two Doppler frequencies, the BER is evaluated for the proposed approach. We also simulate two benchmarks: the conventional benchmark (Conv) applies the linear interpolation [15] for channel estimation and regards ICI as noise in signal detection, the other benchmark (ICI-com) utilizes P-BEM and operates soft ICI compensation in both channel estimation and signal detection [16]. The two benchmarks only use pilot tones to estimate the channels. As mentioned in Section III, we implement channel coding to further enhance the pdf generated in the signal detection phase. Here, the regular repeat accumulate (RA) code with coding rate 1/3 [6] is used.

First, we consider the BPSK modulation, $f/\Delta f$ is configured to be 0.1 for A and B. The BER results of the proposed approach (ICI-aware) are illustrated in Fig. 3. Under different SNR conditions, the BERs are quite stable after 3 iterations, the difference between 4 and 5 iterations is small. Therefore, it verifies that the convergence speed of the proposed approach is fast. The next step is to evaluate the proposed approach under different CFO scenarios. In this study, $f/\Delta f$ is configured to be 0.05 and 0.1, respectively, and both BPSK and QPSK are considered. Notice that $f/\Delta f = 0.1$ is quite a large number in vehicular network according to the 802.11p standard [5] (e.g., relative velocity 200 km/hr would only lead to 0.007 normalized Doppler frequency), and is more than sufficient to evaluate the robustness of the proposed approach. Fig. 4 and 5 demonstrate the BER results. Since Fig. 3 shows that the proposed approach can converge after 5 iterations, Fig. 4 and 5 only show the BER result after 5 iterations for

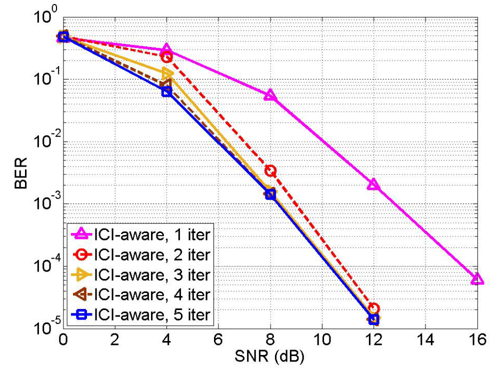

Fig. 3. BER results after different number of iterations (with channel coding).

both the proposed approach and the second benchmark (ICI-com). As can be seen, the proposed approach has better BER

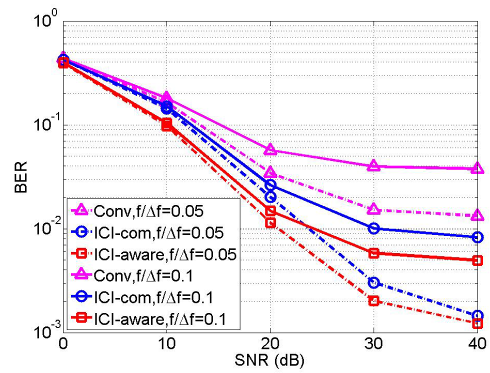

Fig. 4. BER results under BPSK modulation (signal detection).

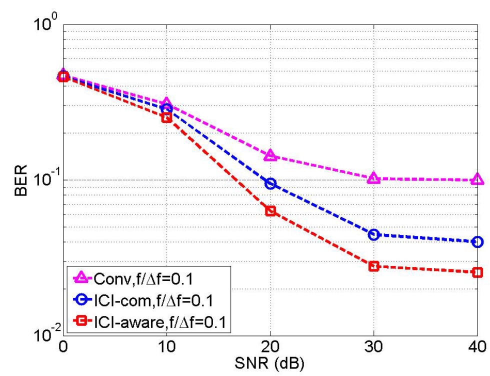

Fig. 5. BER results under QPSK modulation (signal detection).

performances compared with the two benchmarks. In the low SNR regime, the BER results of three methods are relatively close. Then as the SNR increases, the proposed approach shows better BER performances. In most cases, the proposed approach gives more than 2 dB SNR improvement compared with the second best method (ICI-com), and this improvement increases as the SNR increases. The only exception is that the

ICI-com method shows similar performance when BPSK is applied, $f/\Delta f = 0.05$ and SNR is 40 dB. In the high SNR regime, the BER curves of the three methods saturate and the proposed approach offers a lower BER bound. Finally, we consider channel coding and fix the $f/\Delta f$ to be 0.1. Under such configuration, both the BER curves of BPSK and QPSK modulations are illustrated in Fig. 6. For the proposed

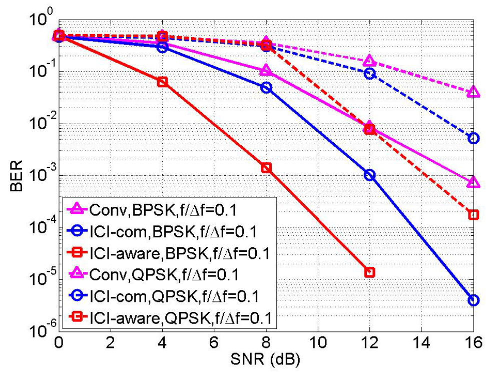

Fig. 6. BER results under different Doppler frequencies (with channel coding).

approach, the BER curve of BPSK begins to drop when SNR = 0 dB and that of QPSK begins to decrease when SNR = 8 dB. Overall, the two curves show low BER in the low SNR regime (e.g., for SNR $<$ 16 dB). Under different modulations, the proposed approach can provide around 4 dB SNR improvement compared with the second best method (ICI-com).

V. Conclusion

Applying PNC to VANETs can potentially boost network throughput to address the intermittent node connectivity and short contact time problems in VANETs. This paper tackles two critical phenomena in PNC VANETs: the CFO between transmitters and receiver, and time-frequency-selective channels. Specifically, we have proposed an ICI-aware approach to mitigate the detrimental effects caused by CFO and time-frequency-selective channels. By exploiting the channel information contained in data tones, it significantly enhances both the channel estimation and signal detection processes. The signal detection part of the approach is implemented with the BP algorithm and the channel estimation part is implemented with the EM algorithm. Both algorithms are ICI-aware. Simulation results indicate that the joint algorithm can converge within 5 iterations. We compare the proposed approach with two benchmarks which are the results of prior schemes [15], [16]. In terms of BER, the approach outperforms two benchmarks , especially in the high SNR regime. We have further considered channel coding, and simulation verifies that the proposed approach provides much lower BER in the low SNR regime compared with the two benchmarks.

Acknowledgment

The work of I. W.-H Ho is supported in part by the Early Career Scheme (Project No. 25200714) established under the University Grant Committee (UGC) of the Hong Kong Special Administrative Region (HKSAR), China; and by The Hong Kong Polytechnic University (Projects G-YBK6, G-YBR2). The work of Z. Situ is partially supported by the National Natural Science Foundation of China (Project No. 61401384). The work of S. C. Liew and T. Wang was supported in part by the Innovation and Technology Fund (Project No. ITF/447/16FP) established under the Innovation and Technology Commission of the Hong Kong Special Administrative Region, China.

References

[1] I. W.-H. Ho, S. C. Liew, and L. Lu, "Feasibility study of physical-layer network coding in 802.11p VANETs," in *2014 IEEE International Symposium on Information Theory*, June 2014, pp. 646–650.

[2] I. W.-H. Ho, R. J. North, J. W. Polak, and K. K. Leung, "Effect of transport models on connectivity of interbus communication networks," *Journal of Intelligent Transportation Systems*, vol. 15, no. 3, pp. 161–178, 2011.

[3] S. Zhang, S. C. Liew, and P. P. Lam, "Hot Topic: Physical-layer Network Coding," in *Proceedings of the 12th Annual International Conference on Mobile Computing and Networking*, ser. MobiCom '06. ACM, 2006, pp. 358–365.

[4] L. F. Xie, I. W.-H. Ho, S. C. Liew, L. Lu, and F. C. M. Lau, "Mitigating Doppler effects on physical-layer network coding in VANET," in *26th IEEE International Symposium on Personal, Indoor, and Mobile Radio Communications (PIMRC)*, Aug 2015, pp. 121–126.

[5] L. F. Xie, I. W. H. Ho, S. C. Liew, L. Lu, and F. C. M. Lau, "The Feasibility of Mobile Physical-Layer Network Coding with BPSK Modulation," *IEEE Transactions on Vehicular Technology*, vol. 66, no. 5, pp. 3976–3990, May 2017.

[6] T. Wang and S. C. Liew, "Joint Channel Estimation and Channel Decoding in Physical-Layer Network Coding Systems: An EM-BP Factor Graph Framework," *IEEE Transactions on Wireless Communications*, vol. 13, no. 4, pp. 2229–2245, April 2014.

[7] L. Lu, T. Wang, S. C. Liew, and S. Zhang, "Implementation of physical-layer network coding," *Physical Communication*, vol. 6, pp. 74–87, 2013.

[8] Z. Wang, J. Huang, S. Zhou, and Z. Wang, "Iterative Receiver Processing for OFDM Modulated Physical-Layer Network Coding in Underwater Acoustic Channels," *IEEE Transactions on Communications*, vol. 61, no. 2, pp. 541–553, February 2013.

[9] M. Wu, F. Ludwig, M. Woltering, D. Wübben, A. Dekorsy, and S. Paul, "Analysis and Implementation for Physical-Layer Network Coding with Carrier Frequency Offset," in *WSA 2014; 18th International ITG Workshop on Smart Antennas*, March 2014, pp. 1–8.

[10] M. Woltering, D. Wübben, and A. Dekorsy, "Physical Layer Network Coding with Gaussian Waveforms using Soft Interference Cancellation," in *IEEE Vehicular Technology Conference (VTC)*, May 2015, pp. 1–5.

[11] M. Pätzold, *Mobile fading channels*. Wiley Online Library, 2002, vol. 14.

[12] T. Wang, S. C. Liew, and L. You, "Joint Phase Tracking and Channel Decoding for OFDM PNC: Algorithm and Experimental Evaluation," in *Proceedings of the 2014 ACM Workshop on Software Radio Implementation Forum*, ser. SRIF '14. ACM, 2014, pp. 69–76.

[13] Z. Tang, R. C. Cannizzaro, G. Leus, and P. Banelli, "Pilot-Assisted Time-Varying Channel Estimation for OFDM Systems," *IEEE Transactions on Signal Processing*, vol. 55, no. 5, pp. 2226–2238, May 2007.

[14] G. Acosta-Marum and M. A. Ingram, "Six time-and frequency-selective empirical channel models for vehicular wireless LANs," *IEEE Vehicular Technology Magazine*, vol. 2, no. 4, pp. 4–11, Dec 2007.

[15] S. Coleri, M. Ergen, A. Puri, and A. Bahai, "Channel estimation techniques based on pilot arrangement in OFDM systems," *IEEE Transactions on Broadcasting*, vol. 48, no. 3, pp. 223–229, Sep 2002.

[16] H. Hijazi and L. Ros, "Polynomial Estimation of Time-Varying Multipath Gains With Intercarrier Interference Mitigation in OFDM Systems," *IEEE Transactions on Vehicular Technology*, vol. 58, no. 1, pp. 140–151, Jan 2009.